NIH Public Access
Author Manuscript
J Neural Eng. Author manuscript; available in PMC 2012 June 1.

Published in final edited form as:
J Neural Eng. 2011 June ; 8(3): 036013. doi:10.1088/1741-2560/8/3/036013.

Decoding rat forelimb movement direction from epidural and intracortical field potentials

Marc W. Slutzky[1,2,3], **Luke R. Jordan**[2], **Eric W. Lindberg**[1], **Kevin E. Lindsay**[4], and **Lee E. Miller**[2,3,5]

[1]Department of Neurology, Northwestern University, Chicago, IL 60611

[2]Department of Physiology, Northwestern University, Chicago, IL 60611

[3]Department of Physical Medicine & Rehabilitation, Northwestern University, Chicago, IL 60611

[4]Department of Biomedical Engineering, Mercer University, Macon, GA 31207

[5]Department of Biomedical Engineering, Northwestern University, Evanston, IL 60603, USA

Abstract

Brain machine interfaces (BMIs) use signals from the brain to control a device such as a computer cursor. Various types of signals have been used as BMI inputs, from single-unit action potentials to scalp potentials. Recently, intermediate-level signals such as subdural field potentials have also shown promise. These different signal types are likely to provide different amounts of information, but we don't yet know what signal types are necessary to enable a particular BMI function, such as identification of reach target location, control of a two-dimensional cursor or the dynamics of limb movement. Here we evaluated the performance of field potentials, measured either intracortically (local field potentials, LFPs) or epidurally (EFPs), in terms of the ability to decode reach direction. We trained rats to move a joystick with their forepaw to control the motion of a sipper tube to one of four targets in two dimensions. We decoded forelimb reach direction from the field potentials using linear discriminant analysis. We achieved a mean accuracy of 69±3% with EFPs and 57±2% with LFPs, both much better than chance. Signal quality remained good up to 13 months after implantation. This suggests that using epidural signals could provide BMI inputs of high quality with less risk to the patient than using intracortical recordings.

Introduction

Brain machine interfaces (BMIs) have the potential to improve the ability of people paralyzed from disorders such as stroke, amyotrophic lateral sclerosis, or spinal cord injury to interact with their environment. In addition to spikes measured intracortically from single neurons [1-4], field potentials representing the summed activity of thousands of neurons have been used as BMI control signals. These field potentials can be recorded from various levels, including the scalp (EEG) [5, 6], below the dura (ECoG) [7-9], and within the cortex (LFPs) [10, 11]. It is generally accepted that there is a trade-off of reduced quality for reduced risk: the less invasive the recording, the lower the signal quality. Spikes tend to be the most informative [4, 12], although one study [13] showed that broadband, multiunit activity (MUA) performed even better than discriminated single spikes at decoding arm trajectories. Although Scherberger et al. [14] showed that LFPs in posterior parietal cortex may predict the intention to move slightly better than do spikes, LFPs generally are

Corresponding author: Marc W. Slutzky, MD, PhD, Dept. of Neurology, Northwestern University, 303 E. Chicago Ave., Ward 5-150, Chicago, IL 60611, mslutzky@md.northwestern.edu.

NIH-PA Author Manuscript
NIH-PA Author Manuscript
NIH-PA Author Manuscript

NIH-PA Author Manuscript

NIH-PA Author Manuscript

NIH-PA Author Manuscript

outperformed by spikes at decoding reaching movements [4, 12, 13]. This difference in decoding may partially be due to greater independence of spikes compared with LFPs. Subdural potentials (ECoG) presumably have the same sources as LFPs but are farther from them, and thus the signal may be reduced. EEG is attenuated dramatically by the CSF, skull, and scalp [15].

It is not yet certain which type of signal is best for a given BMI application. Since intracortical spike recordings can provide highly detailed information about arm kinematics [16], kinetics [17] and muscle activity [18, 19], they have frequently been used as BMI inputs [2, 3, 20]. However, current intracortical electrodes typically record single-unit spikes for no more than 1-3 years [21, 22]. This signal loss is related to various factors, including vascular damage, immune response and neuronal loss [23-26]. Since an LFP is thought to represent the combined activity of hundreds to thousands of neurons [27, 28], it is likely to be more stable than a single unit spike signal [14]. Likewise, multiunit activity (MUA) may be more stable than the activity of single-unit spikes, but it requires high-bandwidth (10-30 kHz) sampling that increases power and processing requirements—important considerations for an eventual implanted device. Finally, spikes, LFPs, and MUA all require intracortical electrodes, which carry increased risk of stroke, hemorrhage, and infection for the patient. Therefore, many groups have begun examining less-invasive signal sources for BMIs.

Subdural signals have recently shown promise as BMI control signals [7, 9, 29, 30]. To date, ECoG-based BMIs have used decoding algorithms that are simple linear combinations of two ECoG features to control a cursor in two [7, 9] dimensions. These algorithms rely on the brain's remarkable plasticity to learn the mapping between, for example, power in the mu (8-13 Hz) band during hand and tongue movement imagery, and cursor movement in two dimensions. Despite this plasticity, many researchers believe that intracortical signals will be necessary to reduce the cognitive load of BMI tasks, or for BMI functions with more degrees of freedom, such as the control of a prosthesis or functional electrical stimulation (FES) of a paralyzed limb. However, several groups have used ECoG offline to decode continuous outputs such as hand trajectories [8, 31-34]. This suggests that more complex BMI functions may be achievable with ECoG, especially if signals more closely related to normal movement are used. Moreover, ECoG may have greater stability than spikes [32]. Thus, ECoG has become a viable contender for a BMI signal source along with intracortical signals.

Epidural field potentials (EFPs) may be similar in quality to ECoG [15] with less risk to the patient from stroke, infection and hemorrhage. While a few preliminary studies have used single, bipolar EFPs in a BMI [29, 35-37], EFPs have not yet been used to decode movement parameters offline, so it is difficult to compare performance in these studies to prior studies using other signals. In this study, we examined the ability to decode reach direction in rats using motor cortical EFPs, and compared this to the decoding performance using LFPs.

Methods

Rat behavior

Behavioral, surgical and recording methods were approved by the Northwestern University Animal Care and Use Committee. Rats were water restricted for approximately 20 hours before each session. After each session, they were allowed at least an hour of unlimited access to water. Each rat was trained to grasp and move a spring-loaded joystick with its left forepaw to guide a sipper tube from one of four positions at 90 degree intervals on the circumference of a circle centered on its mouth. The sipper tube moved in proportion to the joystick position until it came within 3 degrees of the center position, at which point it

NIH-PA Author Manuscript

NIH-PA Author Manuscript

NIH-PA Author Manuscript

stopped, a success tone sounded, and a juice reward was given. One second after the joystick returned to its center position, the sipper tube again moved to one of the 4 outer targets to start the next trial. The rat had 10 seconds in which to move the sipper tube back to the center. Otherwise, the trial was marked as a failure and the next trial began. On average, rats completed trials in 1.2 s. It took an average of 46±11 sessions to train the rats. Details of the behavior are given in[38].

Because we did not restrain the rats during the task, they were able to turn around and often moved their heads at the same time as their forepaws. To assess whether the brain signals we recorded were related to arm or head movement, we trained a subset of the rats on a "reverse task," in which the sipper tube moved in the opposite direction of the joystick for both left/right and up/down axes. Since the rats usually moved their heads along the path of the sipper tube, this reverse task effectively decoupled the movements of the head and forepaw. Rats performed forward and reverse tasks on different days separated by at least a week [38].

Electrode implantation

After rats demonstrated sufficient acquisition of the task (at least 70% of trials were successful, typically 150-200 successful trials per session), we implanted either epidural or intracortical electrodes over the right (contralateral) sensorimotor cortex. The rats were given dexamethasone (0.2 mg/kg IP) 30 min before surgery to reduce brain swelling and atropine (0.05 mg/kg IP) to reduce oral secretions. They were anesthetized using ketamine (100 mg/kg IP) and xylazine (10 mg/kg IP), with supplemental ketamine boluses as needed. Upon recovery from anesthesia, and for two days post-operatively, the rats were given meloxicam (0.2 mg/kg IP) for pain relief and enrofloxacin (5 mg/kg IP) to deter infection. They also received minocycline (0.1 mg/ml) in their water for 2 days prior and 3 days after surgery which has been shown to increase the quality and longevity of neural recordings [39].

We performed a craniectomy centered at the caudal forelimb area, stereotaxic coordinates +1 AP, 2 ML [40, 41]. Three rats were implanted with epidural arrays. Two arrays were custom-built using 100 μm diameter platinum wires embedded in silicone, one 1×16 array with 500 μm interelectrode spacing aligned along the sagittal plane (initially used in [15]), and one 4×4 array with 700 μm spacing. The third array was made from flexible polyimide (4×4, 150 μm contact diameter, 400 μm interelectrode spacing) [42]. We implanted three different rats with 50 μm diameter tungsten microwire electrode arrays (2×8, 250 μm interelectrode spacing, Tucker Davis Technologies). These arrays were placed as close as possible to the stereotaxic coordinates used for the epidural arrays while avoiding large cortical veins, and inserted to a depth of approximately 1.1-1.4 mm. Both epidural and intracortical arrays had similar impedances (~50-150 kΩ measured at 1 kHz). Ground and reference leads were connected to skull screws. The craniectomy was covered with a thin layer of silicone elastomer (Kwik-Cast, World Precision Instruments, Inc., FL) and polymethyl methacrylate acrylic, and the electrode connectors were affixed to the skull with bone screws and acrylic.

Feature extraction

Starting one week after surgery, we recorded field potentials while the rat performed the reaching task. We recorded all signals with an RZ5 Bioamp System (Tucker Davis Technologies [TDT], Alachua, FL), including brain signals, joystick position, digital pulses indicating trial onset, reward, abort, and failure codes. Only successful trials were used in the analysis. Field potentials were band-pass filtered with cutoffs at 2 and 240 Hz and sampled at 500 Hz. We calculated the power within 10 Hz frequency bands relative to that occurring from 1000 ms to 750 ms before movement onset. Power spectra were calculated

NIH-PA Author Manuscript

NIH-PA Author Manuscript

NIH-PA Author Manuscript

with the short-time Fourier transform on Hanning windowed, 256 ms time segments that overlapped by 56 ms (EEGlab Matlab toolbox [43]). As prior studies have shown directional modulation of delta/theta (0-10 Hz) and high gamma (70-170 Hz) bands [12, 44-46], we used the power in these two bands as the features of the signal to use for decoding. The high gamma band was notch filtered at 120 Hz to reduce the line noise harmonic. As features, we used the power in these two bands in two, 256-ms time bins starting 200 ms before movement, and at movement onset. The 64 available features (16 electrodes × 2 time bins × 2 frequency bins) were concatenated into one feature vector.

Feature selection and decoding

We used a one-way ANOVA to rank features in order of the significance of their modulation with movement direction. The z-scores of the most significant features were used to train a linear discriminant analysis (LDA) decoder. We defined decoder performance as the percentage of trials correctly decoded using ten-fold cross-validation. Nine folds were used for training each decoder and the final fold (10% of trials in that session) used for testing; this was repeated 10 times (once for each fold). The mean decoder performance of the 10 folds was used as the performance level for each session. The feature extraction, selection, and decoding sequence is summarized in Figure 1.

Starting with a maximum of 30 features, the relation between number of features and prediction accuracy was examined by iteratively removing the least significant feature and recalculating the accuracy. These feature dropping curves were analyzed to determine the number of features at which the prediction accuracy did not differ significantly from the accuracies using more features. This saturation point was determined by performing a series of one-tailed t-tests comparing performance at each feature number with performance using more features, with $p=0.15$ as the significance threshold [15]. This was repeated for all of the sessions in the study.

The statistical significance of the difference between EFP and LFP decoding performance was evaluated using a mixed model (PROC MIXED, SAS v9.2) with a fixed effect of field potential type and random intercept for animal.

Results

Figure 2(a) demonstrates a rat performing the reaching task with its left forepaw. The joystick is seen on the floor and the sipper tube is mounted in front of the rat. Typical task-related EFPs and behavior signals are shown in panel b. In general, LFPs and EFPs had similar signal amplitudes (50-100 μV). During and slightly before movement, both types of signal increased in high gamma (70-170 Hz) and decreased in mu (8-13 Hz) and beta (13-25 Hz) power. This high-gamma power increase was modulated with reach direction, as seen in the time frequency spectrograms of EFPs (Figure 3(a)) and LFPs (Figure 3(b)).

An example of feature-dropping curves for EFPs and LFPs based on ANOVA feature selection is shown in Figure 4. In this example, EFP and LFP curves saturated at 9 and 12 features, respectively. For both EFPs and LFPs, the high gamma band features tended to be ranked higher than the 0-10 Hz band features. In LFPs, the second time bin (0-256 ms) tended to be ranked higher than the first time bin, but there was no clear temporal pattern for EFPs. Over all sessions, the feature-dropping curves saturated at 8±5 and 10±5 for EFPs and LFPs, respectively. These values were not statistically different ($p=0.4$, Mann-Whitney U test). Consequently, we used the 12 most significant features for prediction of both signal types, and found similar accuracy for EFPs and LFPs.

NIH-PA Author Manuscript

NIH-PA Author Manuscript

NIH-PA Author Manuscript

Figure 5 shows confusion matrices from single sessions for both EFPs and LFPs. In these two sessions, 84 and 125 trials were used to train decoders which achieved an overall accuracy of 74% and 64% for EFPs and LFPs, respectively. Decoding was also consistent across reach directions in these two sessions, with at least 60% accuracy in decoding each direction. A summary of decoding performance for all rats (Figure 6) shows that EFPs decoded with 69±3% accuracy (n=21 sessions from 3 rats, mean ±SE) while LFPs decoded with 57±2% accuracy (n=14 sessions, 3 rats). This difference was not statistically significant (p=0.09, mixed model). The mean number of trials in each session was 107 for EFPs and 161 for LFPs.

Two rats were trained first on the forward (normal) task and then on the reverse task that was designed to decouple head and arm movement. Decoding performance using EFPs remained high in the reverse task, with 65±3% mean accuracy vs. 73±3% mean accuracy on the forward task in these two rats. Time-frequency spectra for one epidural electrode recorded from a rat during both the forward and reverse tasks (8 months apart) are shown in Figures 7(a) and 7(b), respectively. Both forward and reverse tasks had an increase in high gamma power for reaches up and to the left. There was a stronger increase in gamma power in reaches to the right for the reverse task than for the forward task, possibly due to changes in modulation in that electrode during the significant time between these two recordings. It is likely, however, that the modulation in high gamma power was more closely related to forelimb than to head or neck movements. The similarity of high gamma modulation, particularly along the vertical axis, for the forward and reverse tasks was a consistent feature over the great majority of electrodes that modulated during movement for the two rats trained on both tasks. This supports the hypothesis that the high gamma modulation was related to forelimb movements.

The EFP signals retained strong modulation with movement direction for periods in excess of a year (Figure 8). Using decoders rebuilt each day, accuracy remained high out to 400 days in one rat and 250 days in another. This suggests that EFPs are a potentially long-lasting source of signals for reach decoding. Rats implanted with intracortical electrodes were recorded over a time span of less than 6 weeks, (although good LFP decoding in one rat lasted 4 months) so we were unable to assess LFP performance over time.

Discussion

In this study, we have shown that epidural field potentials can be used to decode reaching direction with accuracy that is comparable to that of intracortical field potentials. Both LFPs and EFPs demonstrated increased high gamma (70-170 Hz) power and decreased mu/beta (8-30 Hz) power before and during forelimb movement as has been described in several studies in monkeys [12, 31, 44, 45] and humans [8, 47-49]. The epidural decoding performance of 69% on 4 target directions is comparable or superior to other studies in the literature using subdural field potentials (ECoG) in human subjects [50]or LFPs in monkey M1 [12, 13, 44].

There is considerable variation in the details of these studies: different numbers of targets, different time bins and features used for decoding, different decoders, and different numbers of electrodes, among others. In other studies, performance on 8-target decoding with monkey LFPs ranged from ~45% [44] to 87% [12]. However, the latter study combined data that were recorded sequentially from different electrode locations in M1. This assumed that LFPs were stable across days and that simultaneously recorded LFPs would have the same performance, which may be optimistic for such highly correlated signals [51]. Stark and Abeles [13] reported 53% performance in decoding 6 targets with LFPs, but this included LFPs from both M1 and PMd and used additional information from times before movement

NIH-PA Author Manuscript

NIH-PA Author Manuscript

NIH-PA Author Manuscript

onset. Ball et al. [52] reported 75% mean performance on 4 targets with ECoG in 4 humans. Finally, Mehring et al. [50] compared single electrode performance in human ECoG (35%) and monkey LFPs (49%) in a 4-target reach task.

The present study is the first to compare extracortical and intracortical signal decoding performance directly in the same species, using the same motor task. Moreover, we used electrodes of similar diameter (50 μm and 100 μm) and impedances (~50-150 kΩ at 1 kHz) for both LFP and EFP recording, respectively. Most prior ECoG studies in humans [7, 50, 52] have used larger disc electrodes of at least 2 mm diameter, which translates to 200-400 times the surface area, and much lower impedance, than the electrodes we used. While it is not yet clear what size electrodes are best to record field potentials, our study reduces the effect of some of the extraneous variables in comparing different signal types [50]. While we have shown previously that differences in size and thickness of the cortex and extracortical structures between rats and humans make a large difference in the spatial properties of brain signals in the two species [15], we did not examine the effect of the electrode size. In general, larger electrodes with lower impedances will record from both local and distant (i.e., volume-conducted) signal sources. To record from local sources only, a smaller, higher impedance electrode is probably preferable; however, this requirement must be balanced with the reduced signal-to-noise ratio from higher-impedance electrodes. Our epidural and intracortical arrays had more similar interelectrode spacing than did prior studies of different signal sources (700 μm and 250-500 μm respectively, vs. 10 mm and 350-700 μm for subdural and intracortical electrodes in [50]), which presumably reduced, although did not remove, the effect of spatial resolution on the comparison.

Since we did not restrain the rats, their head and neck tended to move with the sipper tube during the trial. However, we controlled for this using a task that reversed the relation between head and forelimb movements. The high gamma band continued to modulate with forelimb, not head or neck, movement, which increases the likelihood that the signals we decoded were related to forelimb movements.

Since LFPs are recorded in closer proximity to the signal sources than are EFPs, one might have expected better decoding performance with LFPs than with EFPs. Yet our study found an insignificant trend toward better performance with EFPs than with LFPs, although it should be noted that the sample size was rather small. It is possible that the somewhat greater cortical coverage of the epidural arrays compared with intracortical arrays could have improved their performance. Since rats have a small and less well-defined forelimb motor cortex than monkeys, our epidural electrodes might have been more likely to include forelimb movement areas. In any case, EFPs performed about as well as LFPs in rats.

Rats have thinner dura and CSF layers than monkeys and humans, so it is far from certain that in humans, EFPs and LFPs will also perform similarly. We showed previously in rats, that ECoG and EFPs have similar spatial bandwidths [15]. The same study also suggested that human dura has little effect on the field potential signals and that human ECoG and EFP spatial resolutions are similar when the CSF layer is compressed (as it would be with implanted electrodes). Our preliminary evidence from primates also has demonstrated similar performance of EFPs and LFPs on reach direction decoding [53, 54]. Overall, these results suggest that EFPs may provide relatively good performance as BMI inputs for decoding reach direction. They raise the question of whether the performance of EFPs and ECoG performance may also be similar in humans. We are currently examining this possibility using simultaneously recorded ECoG and EFPs in epilepsy patients undergoing preoperative monitoring. If this possibility proves true in humans, EFPs might provide a less-invasive source of signals for BMIs. While there are no studies comparing relative risks of epidural, subdural, and intracortical electrodes in any animal, opening the dura for

NIH-PA Author Manuscript

NIH-PA Author Manuscript

NIH-PA Author Manuscript

subdural or intracortical electrodes likely increases the risks of infection of the brain parenchyma, and could increase the risk of stroke and subdural hemorrhage.

Since field potentials are aggregated from thousands of neurons, it seems plausible that they will be more stable and have greater longevity than will spikes from single neurons. Dickey et al. [55] showed that only 57% of single unit spikes are stable (defined by spike waveform and interspike interval histogram) for one week, and only 39% for 2 weeks. Nicolelis et al. [56] and Jackson and Fetz [57] found similar results at one week and even less stability (10% in the 2007 study) at 2 weeks. In contrast, Chao et al. [32] showed that information decoded from subdural field potentials in monkeys was stable for 250 days. The present study was not designed to assess longevity in either EFPs or LFPs. Technical difficulties (faulty head cap or broken reference wires) limited the duration of recording rather than problems with the electrodes themselves. However, based on the observations in [32] and the results presented here, longer-term testing of subdural and epidural arrays is clearly warranted.

We have demonstrated that EFPs and LFPs perform similarly in decoding intended reach direction in rats, and we have preliminary evidence to suggest similar performance in monkeys [53]. However, it remains to be seen whether EFPs can perform as well as LFPs at decoding more complex signals such as the time course of hand movement, endpoint force, or EMG. We are currently investigating these properties in monkeys. Determining the capabilities of particular signal sources in terms of various BMI functions is an important step toward translating BMIs to clinical use. For example, EFPs might suffice to implement target selection for a patient with locked-in syndrome from amyotrophic lateral sclerosis, but to implement BMI-controlled FES in a patient with tetraplegia from a spinal cord injury, it may be necessary to use spikes. Ultimately, matching input signals to desired BMI functions could allow clinicians more flexibility in selecting a BMI to match each patient's needs while minimizing risk.

References

1. Pesaran B, Pezaris JS, Sahani M, Mitra PP, Andersen RA. Temporal structure in neuronal activity during working memory in macaque parietal cortex. Nat Neurosci. 2002; 5:805–11. [PubMed: 12134152]
2. Serruya MD, Hatsopoulos NG, Paninski L, Fellows MR, Donoghue JP. Instant neural control of a movement signal. Nature. 2002; 416:141–2. [PubMed: 11894084]
3. Taylor DM, Tillery SI, Schwartz AB. Direct cortical control of 3D neuroprosthetic devices. Science. 2002; 296:1829–32. [PubMed: 12052948]
4. Wessberg J, Stambaugh CR, Kralik JD, Beck PD, Laubach M, Chapin JK, Kim J, Biggs SJ, Srinivasan MA, Nicolelis MA. Real-time prediction of hand trajectory by ensembles of cortical neurons in primates. Nature. 2000; 408:361–5. [PubMed: 11099043]
5. Birbaumer N, Ghanayim N, Hinterberger T, Iversen I, Kotchoubey B, Kubler A, Perelmouter J, Taub E, Flor H. A spelling device for the paralysed. Nature. 1999; 398:297–8. [PubMed: 10192330]
6. Wolpaw JR, McFarland DJ. Control of a two-dimensional movement signal by a noninvasive brain-computer interface in humans. Proc Natl Acad Sci U S A. 2004; 101:17849–54. [PubMed: 15585584]
7. Leuthardt EC, Schalk G, Wolpaw JR, Ojemann JG, Moran DW. A brain-computer interface using electrocorticographic signals in humans. J Neural Eng. 2004; 1:63–71. [PubMed: 15876624]
8. Schalk G, Kubanek J, Miller KJ, Anderson NR, Leuthardt EC, Ojemann JG, Limbrick D, Moran D, Gerhardt LA, Wolpaw JR. Decoding two-dimensional movement trajectories using electrocorticographic signals in humans. J Neural Eng. 2007; 4:264–75. [PubMed: 17873429]
9. Felton EA, Wilson JA, Williams JC, Garell PC. Electrocorticographically controlled brain-computer interfaces using motor and sensory imagery in patients with temporary subdural electrode implants. Report of four cases. J Neurosurg. 2007; 106:495–500. [PubMed: 17367076]

NIH-PA Author Manuscript

NIH-PA Author Manuscript

NIH-PA Author Manuscript

10. Kennedy PR, Kirby MT, Moore MM, King B, Mallory A. Computer control using human intracortical local field potentials. IEEE Trans Neural Syst Rehabil Eng. 2004; 12:339–44. [PubMed: 15473196]
11. Hwang EJ, Andersen RA. Brain Control of Movement Execution Onset Using Local Field Potentials in Posterior Parietal Cortex. J Neurosci. 2009; 29:14363. [PubMed: 19906983]
12. Mehring C, Rickert J, Vaadia E, Cardosa de Oliveira S, Aertsen A, Rotter S. Inference of hand movements from local field potentials in monkey motor cortex. Nat Neurosci. 2003; 6:1253–4. [PubMed: 14634657]
13. Stark E, Abeles M. Predicting movement from multiunit activity. J Neurosci. 2007; 27:8387–94. [PubMed: 17670985]
14. Scherberger H, Jarvis MR, Andersen RA. Cortical local field potential encodes movement intentions in the posterior parietal cortex. Neuron. 2005; 46:347–54. [PubMed: 15848811]
15. Slutzky MW, Jordan LR, Krieg T, Chen M, Mogul DJ, Miller LE. Optimal spacing of surface electrode arrays for brain-machine interface applications. J Neural Eng. 2010; 7:26004. [PubMed: 20197598]
16. Georgopoulos A, Kalaska J, Caminiti R, Massey J. On the relations between the direction of two-dimensional arm movements and cell discharge in primate motor cortex. J Neurosci. 1982; 2:1527–37. [PubMed: 7143039]
17. Evarts EV, Fromm C, Kroller J, Jennings VA. Motor cortex control of finely graded forces. J Neurophysiol. 1983; 49:1199. [PubMed: 6864246]
18. Morrow MM, Miller LE. Prediction of muscle activity by populations of sequentially recorded primary motor cortex neurons. J Neurophysiol. 2003; 89:2279–88. [PubMed: 12612022]
19. Pohlmeyer EA, Solla SA, Perreault EJ, Miller LE. Prediction of upper limb muscle activity from motor cortical discharge during reaching. J Neural Eng. 2007; 4:11.
20. Carmena JM, Lebedev MA, Crist RE, O'Doherty JE, Santucci DM, Dimitrov DF, Patil PG, Henriquez CS, Nicolelis MA. Learning to control a brain-machine interface for reaching and grasping by primates. PLoS biology. 2003; 1:E42. [PubMed: 14624244]
21. Suner S, Fellows MR, Vargas-Irwin C, Nakata GK, Donoghue JP. Reliability of signals from a chronically implanted, silicon-based electrode array in non-human primate primary motor cortex. IEEE Trans Neural Syst Rehabil Eng. 2005; 13:524. [PubMed: 16425835]
22. Hochberg LR, Serruya MD, Friehs GM, Mukand JA, Saleh M, Caplan AH, Branner A, Chen D, Penn RD, Donoghue JP. Neuronal ensemble control of prosthetic devices by a human with tetraplegia. Nature. 2006; 442:164–71. [PubMed: 16838014]
23. Turner JN, Shain W, Szarowski DH, Andersen M, Martins S, Isaacson M, Craighead H. Cerebral Astrocyte Response to Micromachined Silicon Implants. Exp Neurol. 1999; 156:33–49. [PubMed: 10192775]
24. Williams JC, Rennaker RL, Kipke DR. Long-term neural recording characteristics of wire microelectrode arrays implanted in cerebral cortex. Brain Research Protocols. 1999; 4:303–13. [PubMed: 10592339]
25. Biran R, Martin DC, Tresco PA. Neuronal cell loss accompanies the brain tissue response to chronically implanted silicon microelectrode arrays. Exp Neurol. 2005; 195:115–26. [PubMed: 16045910]
26. Polikov VS, Tresco PA, Reichert WM. Response of brain tissue to chronically implanted neural electrodes. J Neurosci Methods. 2005; 148:1–18. [PubMed: 16198003]
27. Mitzdorf U. Properties of the evoked potential generators: current source-density analysis of visually evoked potentials in the cat cortex. Int J Neurosci. 1987; 33:33–59. [PubMed: 3610492]
28. Logothetis NK. The underpinnings of the BOLD functional magnetic resonance imaging signal. J Neurosci. 2003; 23:3963. [PubMed: 12764080]
29. Leuthardt EC, Miller KJ, Schalk G, Rao RP, Ojemann JG. Electrocorticography-based brain computer interface--the Seattle experience. IEEE Trans Neural Syst Rehabil Eng. 2006; 14:194–8. [PubMed: 16792292]
30. Schalk G, Miller KJ, Anderson NR, Wilson JA, Smyth MD, Ojemann JG, Moran DW, Wolpaw JR, Leuthardt EC. Two-dimensional movement control using electrocorticographic signals in humans. J Neural Eng. 2008; 5:75–84. [PubMed: 18310813]

NIH-PA Author Manuscript

NIH-PA Author Manuscript

NIH-PA Author Manuscript

31. Rickert J, Oliveira SC, Vaadia E, Aertsen A, Rotter S, Mehring C. Encoding of movement direction in different frequency ranges of motor cortical local field potentials. J Neurosci. 2005; 25:8815–24. [PubMed: 16192371]
32. Chao ZC, Nagasaka Y, Fujii N. Long-term asynchronous decoding of arm motion using electrocorticographic signals in monkeys. Front Neuroeng. 2010; 3
33. Gunduz A, Sanchez JC, Carney PR, Principe JC. Mapping broadband electrocorticographic recordings to two-dimensional hand trajectories in humans ⁜ Motor control features. Neural Networks. 2009; 22:1257–70. [PubMed: 19647981]
34. Ganguly K, Secundo L, Ranade G, Orsborn A, Chang EF, Dimitrov DF, Wallis JD, Barbaro NM, Knight RT, Carmena JM. Cortical representation of ipsilateral arm movements in monkey and man. J Neurosci. 2009; 29:12948. [PubMed: 19828809]
35. Rouse AG, Heldman DA, Moran DW. Neural adaptation of epidural electrocorticographic (EECoG) signals during closed-loop brain computer interface (BCI) control. Soc for Neuroscience Annual Meeting Abstract. 2007
36. Kennedy P, Andreasen D, Ehirim P, King B, Kirby T, Mao H, Moore M. Using human extra-cortical local field potentials to control a switch. J Neural Eng. 2004; 1:72–7. [PubMed: 15876625]
37. Sutter EE. The brain response interface: communication through visually induced electrical brain responses. Journal of Microcomputer Applications. 1992; 15:31–45.
38. Slutzky MW, Jordan LR, Bauman MJ, Miller LE. A new rodent behavioral paradigm for studying forelimb movement. J Neurosci Methods. 2010; 192:228–32. [PubMed: 20691727]
39. Rennaker RL, et al. Minocycline increases quality and longevity of chronic neural recordings. J Neural Eng. 2007; 4:L1. [PubMed: 17409469]
40. Neafsey EJ, Bold EL, Haas G, Hurley-Gius KM, Quirk G, Sievert CF, Terreberry RR. The organization of the rat motor cortex: a microstimulation mapping study. Brain Res Reviews. 1986; 11:77–96.
41. Hyland B. Neural activity related to reaching and grasping in rostral and caudal regions of rat motor cortex. Behav Brain Res. 1998; 94:255–69. [PubMed: 9722277]
42. Kim J, Wilson JA, Williams JC. A cortical recording platform utilizing microECoG electrode arrays. 2007:5353.
43. Delorme A, Makeig S. EEGLAB: an open source toolbox for analysis of single-trial EEG dynamics including independent component analysis. J Neurosci Methods. 2004; 134:9–21. [PubMed: 15102499]
44. O'Leary JG, Hatsopoulos NG. Early visuomotor representations revealed from evoked local field potentials in motor and premotor cortical areas. J Neurophysiol. 2006; 96:1492. [PubMed: 16738219]
45. Heldman DA, Wang W, Chan SS, Moran DW. Local field potential spectral tuning in motor cortex during reaching. IEEE Trans Neural Syst Rehabil Eng. 2006; 14:180–3. [PubMed: 16792288]
46. Miller KJ, Leuthardt EC, Schalk G, Rao RP, Anderson NR, Moran DW, Miller JW, Ojemann JG. Spectral changes in cortical surface potentials during motor movement. J Neurosci. 2007; 27:2424–32. [PubMed: 17329441]
47. Pfurtscheller G, Lopes da Silva FH. Event-related EEG/MEG synchronization and desynchronization: basic principles. Clin Neurophysiol. 1999; 110:1842–57. [PubMed: 10576479]
48. Graimann B, Huggins JE, Levine SP, Pfurtscheller G. Visualization of significant ERD/ERS patterns in multichannel EEG and ECoG data. Clin Neurophysiol. 2002; 113:43–7. [PubMed: 11801423]
49. Acharya S, Fifer MS, Benz HL, Crone NE, Thakor NV. Electrocorticographic amplitude predicts finger positions during slow grasping motions of the hand. J Neural Eng. 2010; 7:046002. [PubMed: 20489239]
50. Mehring C, Nawrot MP, de Oliveira SC, Vaadia E, Schulze-Bonhage A, Aertsen A, Ball T. Comparing information about arm movement direction in single channels of local and epicortical field potentials from monkey and human motor cortex. J Physiol Paris. 2004; 98:498–506. [PubMed: 16310349]

NIH-PA Author Manuscript

NIH-PA Author Manuscript

NIH-PA Author Manuscript

51. Gilja V, Yu BM, Santhanam G, Afshar A, Ryu SI, Shenoy KV. Factor analysis based BCI decoding from spikes and LFP. Society for Neuroscience Annual Meeting. 2008

52. Ball T, Schulze-Bonhage A, Aertsen A, Mehring C. Differential representation of arm movement direction in relation to cortical anatomy and function. J Neural Eng. 2009; 6:16006.

53. Slutzky MW, Jordan LR, Miller LE. Evaluation of epidural and intracortical field potentials as control inputs for brain-machine interfaces. Society for Neuroscience Annual Meeting Abstracts. 2009

54. Slutzky MW, Lindberg E, Jordan LR, Miller LE. Decoding motor outputs with epidural and intracortical inputs: performance similarities and differences. Society for Neuroscience Annual Meeting Abstracts. 2010

55. Dickey AS, Suminski A, Amit Y, Hatsopoulos NG. Single-unit stability using chronically implanted multielectrode arrays. J Neurophysiol. 2009; 102:1331–9. [PubMed: 19535480]

56. Nicolelis MA, Dimitrov D, Carmena JM, Crist R, Lehew G, Kralik JD, Wise SP. Chronic, multisite, multielectrode recordings in macaque monkeys. Proc Natl Acad Sci U S A. 2003; 100:11041–6. [PubMed: 12960378]

57. Jackson A, Fetz EE. Compact movable microwire array for long-term chronic unit recording in cerebral cortex of primates. J Neurophysiol. 2007; 98:3109–18. [PubMed: 17855584]

NIH-PA Author Manuscript

NIH-PA Author Manuscript

NIH-PA Author Manuscript

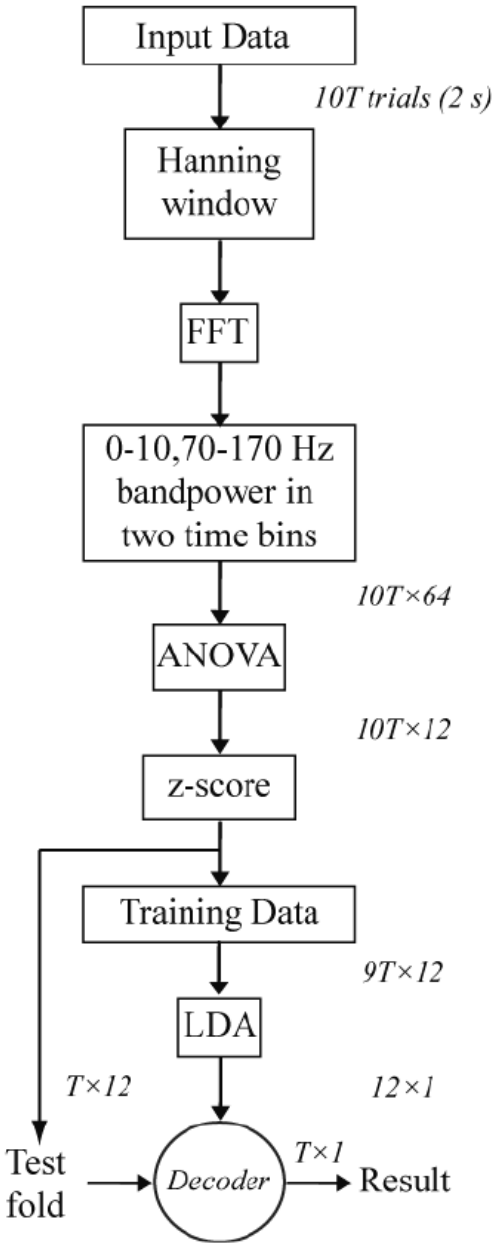

Figure 1.
Flow chart for feature extraction, selection, and decoding. Dimensions at each step are shown to the right or above the arrows. *T*, number of trials in one fold of cross-validation. The sequence from z-score to Result is repeated 10 times, once for each fold, and the results averaged to define the performance of each session.

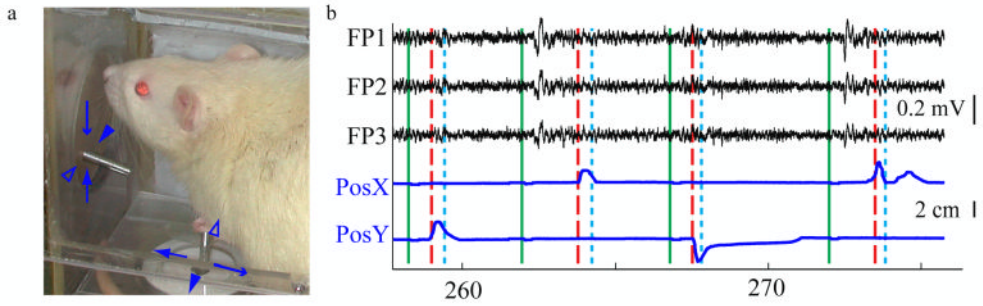

Figure 2.

Rat performing reaching task. (a) The rat moves the joystick to move the sipper tube. The different arrows and arrowheads denote the corresponding joystick and sipper tube movements in each direction. The corresponding forepaw positions and epidural field potentials are shown in (b). Occurrences of go cues, movement onset, and rewards are displayed as green, red dashed, and cyan dotted lines, respectively. Joystick position signals (X and Y for left/right and up/down movements respectively) are shown in the bottom two traces (blue).

NIH-PA Author Manuscript
NIH-PA Author Manuscript
NIH-PA Author Manuscript

NIH-PA Author Manuscript

NIH-PA Author Manuscript

NIH-PA Author Manuscript

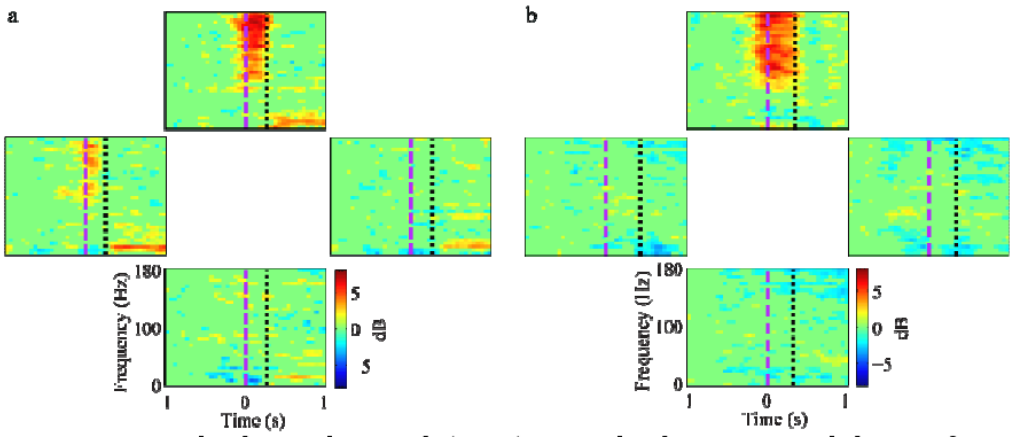

Figure 3.

Event-related spectral potentials (ERSP) averaged with respect to reach direction for a single (a) epidural and (b) intracortical electrode. Each plot shows the average ERSP (in units of log spectral power relative to the -1 to -0.75 s baseline) over all trials to that direction. Plots are spatially arranged in the direction of the reach (up, down, left, and right). In these examples, both EFPs and LFPs show increased high gamma power for reaches in the up direction, with the EFP also showing some increased power in reaches to the left. These changes started slightly before movement onset (purple dashed lines) and ended at movement offset (black dotted lines).

NIH-PA Author Manuscript
NIH-PA Author Manuscript
NIH-PA Author Manuscript

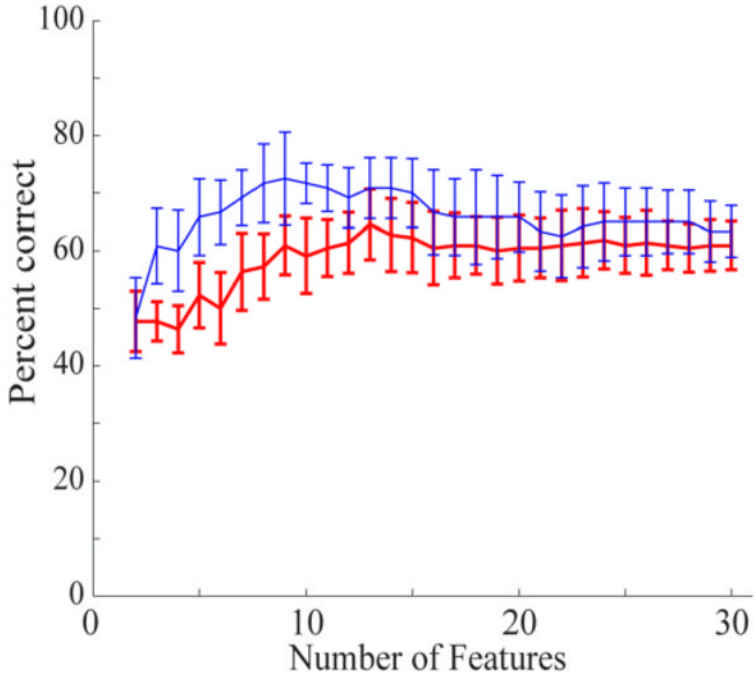

Figure 4.

Feature-dropping curves using ANOVA feature selection for one session of EFP (thin blue line) and LFP recordings (thick red line). The highest-ranked features were dropped last. The EFP curve saturates at about 9 features while the LFP curve saturates at about 12 features. Error bars show standard deviation for 10-fold cross-validation.

NIH-PA Author Manuscript

NIH-PA Author Manuscript

NIH-PA Author Manuscript

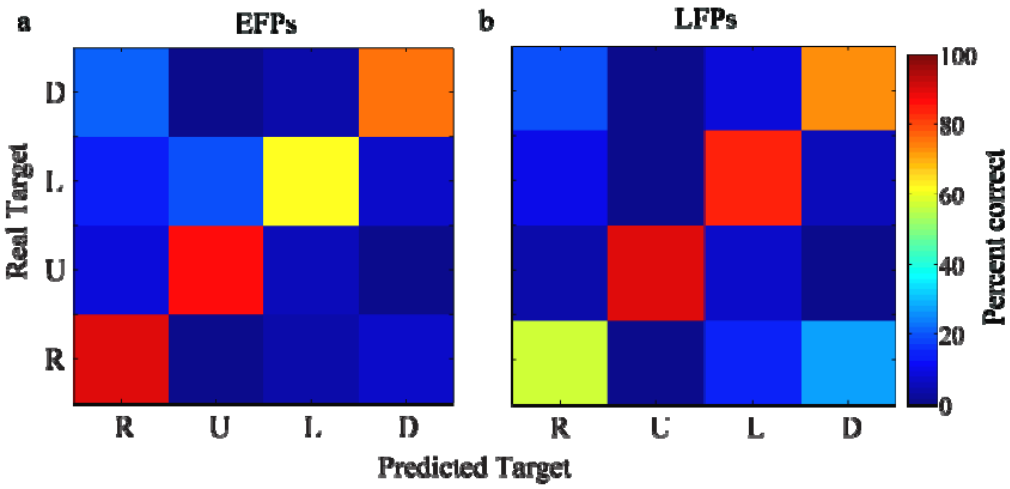

Figure 5.
Confusion matrices of decoded and actual data from one session using (a) epidural field potentials (EFPs) and (b) local field potentials (LFPs).

NIH-PA Author Manuscript
NIH-PA Author Manuscript
NIH-PA Author Manuscript

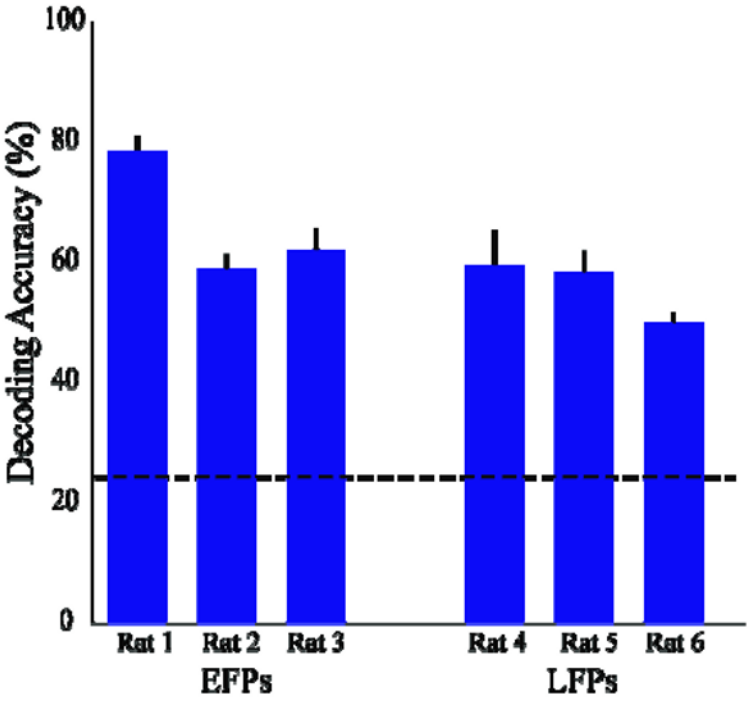

Figure 6.
Summary of decoding performance for EFPs and LFPs over all sessions for each rat. Error bars denote standard errors. Chance prediction was 25% (dashed line). EFP and LFP performance did not significantly differ.

NIH-PA Author Manuscript

NIH-PA Author Manuscript

NIH-PA Author Manuscript

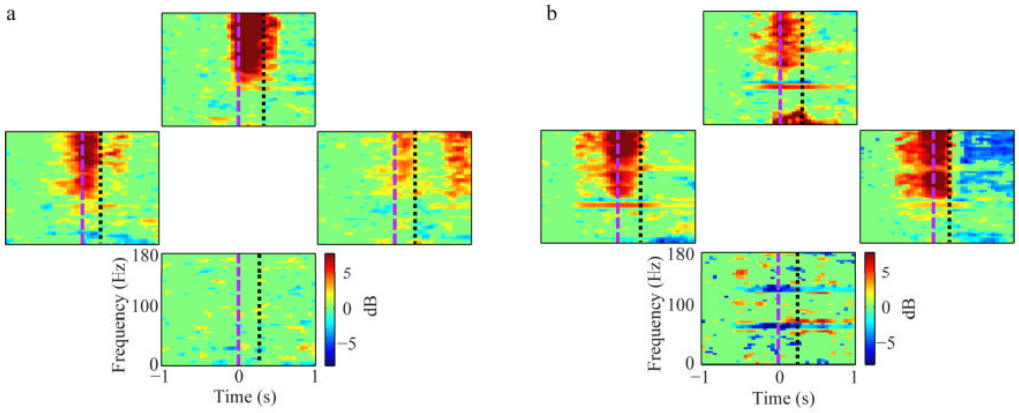

Figure 7.

Event-related spectral potentials (ERSP) averaged to reach direction for EFPs recorded from the same electrode during (a) forward and (b) reverse tasks. Power increases in the high gamma band (70-170 Hz) starting just before movement onset (purple dashed line) are evident in reaches to the upper, left and right directions in both tasks. This suggests that recorded signals in this electrode are related to reach direction, not head movement direction.

NIH-PA Author Manuscript
NIH-PA Author Manuscript
NIH-PA Author Manuscript

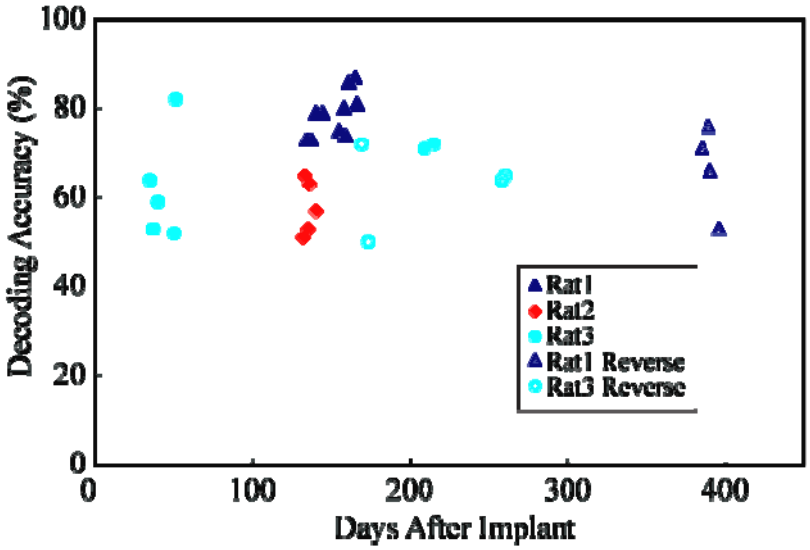

Figure 8.

Decoding accuracy of EFPs remains stable over time. Performance on both forward (closed symbols) and reverse (open symbols) tasks are shown for 3 rats (only 2 rats on reverse task). Decoders for each session were rebuilt on each session's data.